A Comparative Analysis of Krylov Solvers for Three-Dimensional Simulations of Borehole Sensors

Marcela S. Novo, Luiz C. da Silva, and Fernando L. Teixeira, *Senior Member, IEEE*

***Abstract*—We perform a comparative analysis of three Krylov subspace methods, viz., the restarted generalized minimum residual (RGMRES), the conjugate gradient squared (CGS), and the stabilized biconjugate gradient (Bi-CGSTAB), for solving large non-Hermitian sparse linear systems arising from the 3-D finite-volume modeling of electromagnetic borehole sensors in complex earth formations. Incomplete LU factorization and symmetric successive overrelaxation preconditioning strategies are used to speed up the convergence rate. We compare these algorithms in terms of accuracy, convergence rate, and overall CPU time. Results show that CGS has a highly irregular convergence behavior, whereas RGMRES and Bi-CGSTAB provide similar numerical accuracy. However, the convergence rate and CPU time of the latter depend on the borehole sensor geometry and on the type of preconditioner adopted.**

***Index Terms*—Borehole sensors, finite volume, iterative methods, well logging.**

I. Introduction

THE ANALYSIS of electromagnetic borehole sensors in complex earth formations plays an important role for a number of remote sensing applications. Logging-while-drilling sensors, for example, are instrumental in the detection of resistive bed boundaries and characterization of hydrocarbon-rich zones [1]–[4]. Over the years, several numerical methods have been employed to study the electromagnetic response of borehole sensors [5]–[17]. In particular, a robust 3-D finite-volume technique based on coupled vector–scalar potentials has recently been successfully applied to simulate resistivity logging-while-drilling sensors in complex 3-D formations with anisotropic layers [18]–[20].

Similar to other frequency-domain methods, the finite-volume method yields a sparse linear system. For large problems, it is necessary to employ iterative solvers. In earth formations with conductive beds, the resulting system matrix A is complex symmetric but non-Hermitian and indefinite. As a result, the well-known conjugate gradient (CG) method is not suited. Krylov subspace methods are known to perform well for a wide range of applications involving non-Hermitian systems, along with suitable preconditioners to improve convergence [21].

In general, it is not a simple task to recommend one iterative method over another because the number of iterations required for convergence is not usually known in advance. This number depends on the required accuracy and on properties of A—its sparsity pattern and eigenvalue distribution, and particularly its condition number. For the class of problems considered here, A is typically ill-conditioned, so the convergence also depends on the right-hand side (RHS).

In this letter, we study the convergence rate of some state-of-the-art Krylov subspace methods, viz., restarted generalized minimum residual (RGMRES), conjugate gradient squared (CGS), and stabilized biconjugate gradient (Bi-CGSTAB), for solving large non-Hermitian sparse linear systems arising from the finite-volume modeling of electromagnetic logging-while-drilling sensor tools in 3-D borehole environments using coupled scalar–vector potentials. Incomplete LU (ILU) factorization and symmetric successive overrelaxation (SSOR) are used as a preconditioner to accelerate the convergence rate. We assess these methods in terms of their relative accuracy, convergence rate, and overall CPU time. Numerical results show that CGS presents a highly irregular convergence behavior, while RGMRES and Bi-CGSTAB provide accurate results in complex borehole environments, such as those including deviated boreholes and inhomogeneous formations. Although RGMRES and Bi-CGSTAB are competitive in terms of numerical accuracy, their convergence rate and CPU time depend on the sensor geometry and on the type of preconditioning strategy adopted.

II. Formulation

The finite-volume technique considered here is based on a coupled scalar–vector potential formulation where the Helmholtz decomposition is applied to the electric field. This is done to mitigate the ill-conditioning caused by the nontrivial null space of the discrete curl operator. Details on the logging sensor geometry considered and the coupled scalar–vector potential formulation employed here can be found in [20, Sec. II].

Manuscript received September 22, 2009; revised December 10, 2009 and March 29, 2010; accepted May 12, 2010. Date of publication July 26, 2010; date of current version December 27, 2010. This work was supported in part by a Fundação de Amparo à Pesquisa do Estado do Rio de Janeiro Fellowship and in part by the Ohio Supercomputer Center under Grant PAS-0061.

M. S. Novo is with the Department of Electrical Engineering, Federal University of Bahia, Salvador 40210-630, Brazil (e-mail: marcela.novo@ufba.br).

L. C. da Silva is with the Center for Telecommunication Studies and Department of Electrical Engineering, Pontifical Catholic University of Rio de Janeiro, Rio de Janeiro 22453-900, Brazil (e-mail: lcosta@cetuc.puc-rio.br).

F. L. Teixeira is with the ElectroScience Laboratory and Department of Electrical and Computer Engineering, The Ohio State University, Columbus, OH 43212 USA (e-mail: teixeira@ece.osu.edu).

Color versions of one or more of the figures in this paper are available online at http://ieeexplore.ieee.org.

Digital Object Identifier 10.1109/LGRS.2010.2051941

After the finite-volume discretization, a sparse linear system is obtained

$$Ax = b \tag{1}$$

where A is a complex non-Hermitian matrix, x is the vector of unknowns corresponding to the discrete scalar and vector potentials, and b is the discrete source representation.

For a typical 3-D logging sensor simulation with a grid of $50 \times 10 \times 300$ cells, there are over 600 000 complex unknowns to determine, which calls for an iterative solution method.

Many of the most effective iterative methods for the solution of (1) can be classified as nonstationary Krylov subspace methods [21]. For complex non-Hermitian matrices, this includes RGMRES(m), CGS, and Bi-CGSTAB(ℓ) methods [21], [22].

RGMRES(m) is based on the Arnoldi method [23], which explicitly generates an orthogonal basis for the Krylov subspace span$\{A^k r_0\}$, for $k = 0, 1, 2, \ldots$, where r_0 is the initial residual. The solution is then expanded onto the orthogonal basis so as to minimize the residual norm. The generation of the basis requires a "long" recurrence relation, resulting in prohibitive computational and storage costs. RGMRES(m) limits these costs by restarting the Arnoldi process from the latest available residual every m iterations. The value of m is chosen in advance and is fixed throughout the computation. Unfortunately, an optimum value of m cannot easily be predicted.

CGS is a development of the biconjugate gradient method (Bi-CG) where two biorthogonal sequences of vectors are generated. Unlike Bi-CG, CGS applies update operations for the A and A^T sequences both to the same vectors. Ideally, this would speed up the convergence rate by two, but in practice, convergence may be much more irregular than for Bi-CG. A practical advantage is that actual multiplications by A^T are avoided.

Bi-CGSTAB(ℓ) is a variant of Bi-CG (like CGS) but using different updates for the A^T sequence in order to obtain smoother convergence than CGS. Two main steps can be identified for each iteration: an orthogonal-residual step where a basis of order ℓ is generated by a Bi-CG iteration and a minimum-residual step where the residual is minimized over the basis generated, by an approach akin to GMRES. For $\ell = 1$, the method corresponds to the Bi-CGSTAB method of Van der Vorst [24]. For $\ell > 1$, more information about complex eigenvalues of the iteration matrix can be taken into account, and this may lead to improved convergence and robustness. However, as ℓ increases, numerical instabilities may arise.

It is well known that faster convergence can be achieved using a preconditioner. Here, we consider ILU factorization and SSOR preconditioners [21], [22]. The amount of fill-in occurring in the incomplete factorization is controlled by means of the drop tolerance DTOL, i.e., the value below which elements are taken as zero. A potential fill-in element a_{ij} occurring in row i and column j will not be included if $|a_{ij}| < \text{DTOL} \times \alpha$, where α is the maximum modulus element in the matrix A. Complete pivoting by rows for sparsity and by columns for stability is adopted here.

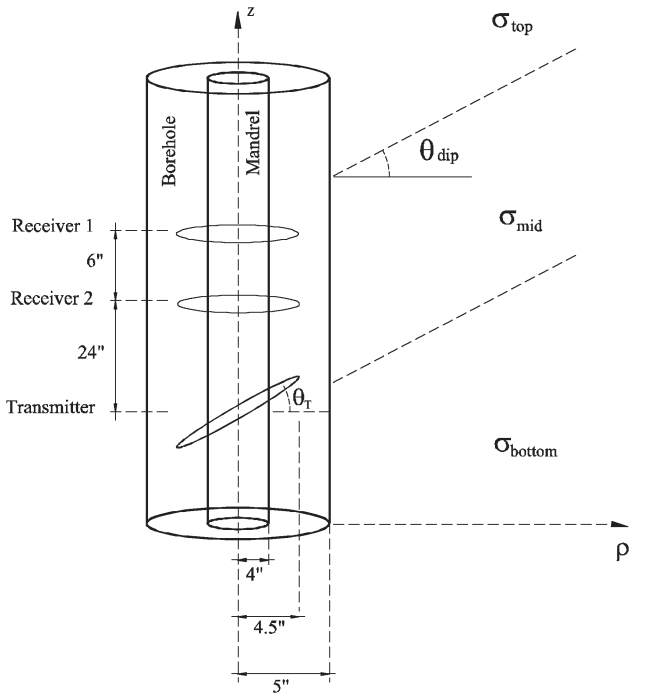

Fig. 1. Prototypical 2-MHz logging-while-drilling sensor tool crossing an earth formation with a dipping bed.

III. Results

In our analysis, we consider a prototypical 2-MHz logging-while-drilling sensor geometry having one transmitter coil (loop) antenna and two receiver coil antennas, as shown in Fig. 1. The antennas are wrapped around a cylindrical steel mandrel of radius 4 in. The coil antennas themselves have radii equal to 4.5 in. The center of the transmitter antenna is chosen as $z = 0$ in. The two receiver antennas are located 30 and 24 in away from the center of the transmitter antenna. The sensor tool resides in a 5-in borehole radius filled with an oil-based mud, with conductivity $\sigma_{\text{mud}} = 5 \times 10^{-4}$ S/m. The parameters of interest are the phase difference (PD) and the amplitude ratio (AR) between the voltages induced at the two receiver antennas. Two surrounding earth formations are considered: 1) homogeneous formation and 2) 45° deviated borehole in inhomogeneous formation.

For both scenarios, we simulate conventional ($\theta_T = 0^\circ$) and directional ($\theta_T = 45^\circ$) sensors. Here, θ_T refers to the axial tilt angle of the tilted-coil transmitter antenna (see Fig. 1). The receiver loop antennas are always horizontal (no tilt). The system matrix A depends on the frequency of operation and earth formation properties only, and it remains the same whether a conventional or a directional sensor is considered. However, the RHS changes according to the transmitter antenna angle. The solution of the linear system often absorbs more than 90% of the overall CPU time of the numerical finite-volume simulation. The following termination criterion is adopted for the iterative solvers:

$$\|\bar{r}_k\|_2 \leq \tau \left(\|\bar{r}_0\|_2 + \sigma_1(\bar{A}) \|\Delta \bar{x}_k\|_2 \right) \tag{2}$$

where $\sigma_1(\bar{A})$ is the largest singular value of the (preconditioned) iteration matrix $\bar{A}$ and τ denotes a specified tolerance.

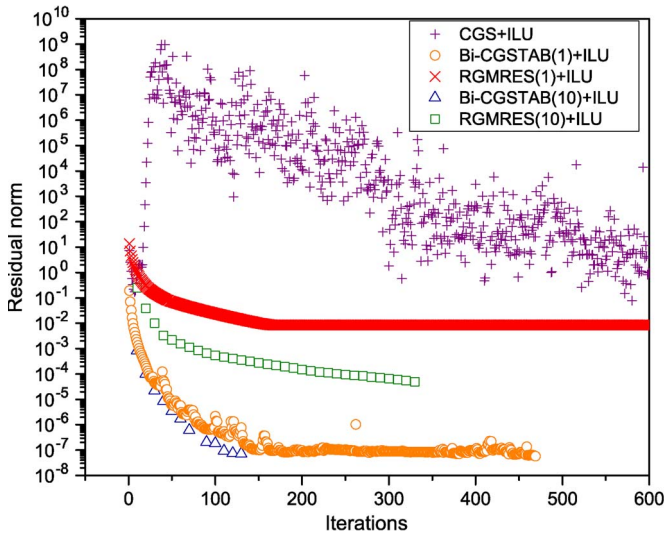

Fig. 2. Performance of preconditioned CGS, Bi-CGSTAB, and RGMRES. Homogeneous formation with mud-filled borehole case.

The iteration process stops when a relative accuracy of 10^{-6} is achieved or when the number of iterations exceeded 70 000. Simulations are carried out on an IBM system with 2.6-GHz AMD Opteron processor.

First, we consider a homogeneous formation with mud-filled borehole. The formation has conductivity equal to 1.0 S/m. The computational domain is discretized using a nonuniform cylindrical grid with $(N_\rho, N_\varphi, N_z) = (49, 30, 419)$ cells, where $\Delta\rho$ varies from 0.635 cm close to the mandrel to 7.12 cm at the outer end and Δz varies slightly from 0.635 cm nearby the coil antennas to 0.641 cm far from them. A cylindrical grid is used to better conform to the geometry of the sensor tool. A nonuniform grid is adopted along the ρ- and z-directions to reduce overall memory requirements for a given physical size domain. The finite-volume discretization leads to 2 421 660 unknowns in the solution vector x and a total of 24 608 790 nonzero elements in the system matrix A. In this example, a relatively fine grid is chosen, but in practice, coarser grids can be employed depending on the required accuracy, leading to faster simulation times (see Fig. 4). The convergence behavior of Bi-CGSTAB(ℓ), RGMRES(m), and CGS for this example is shown in Fig. 2. In this case, ILU is used as a preconditioner and DTOL is set to 10^{-4}. It should be mentioned that, without preconditioning, all methods have failed for this example. Results show that Bi-CGSTAB(1) algorithm converges slowly, whereas RGMRES(1) stagnates and CGS presents wild oscillations in the residual norm that degrade the numerical performance. Bi-CGSTAB(10) converges rather smoothly and is also often faster than RGMRES(10).

In order to better analyze the performance of Bi-CGSTAB(ℓ) and RGMRES(m), the number of iterations and CPU time as a function of the order ℓ of the Bi-CGSTAB(ℓ) polynomial are summarized in Tables I and II, for conventional and directional sensor simulations, respectively. Similarly, Tables III and IV show results as a function of the dimension m of the restart subspace of RGMRES(m). Finite-volume results were validated against pseudoanalytical results [20]. It is observed that, for both conventional and directional sensor simulations,

TABLE I
CONVERGENCE OF Bi-CGSTAB(ℓ) + ILU: CONVENTIONAL SENSOR ($\theta_T = 0°$)/PSEUDOANALYTICAL RESULTS [20]: AR = 2.37753 AND PD = 22.51453

ℓ	Iterations	CPU time (s)	$\|\bar{r}_k\|_2$	AR	PD
1	470	3879	5.739E-8	2.37213	22.02277
3	204	1946	5.751E-8	2.37212	22.02277
5	150	1446	5.599E-8	2.37212	22.02286
7	140	1363	5.835E-8	2.37211	22.02258
9	135	1327	5.750E-8	2.37213	22.02319
10	140	1375	5.343E-8	2.37213	22.02280

TABLE II
CONVERGENCE OF Bi-CGSTAB(ℓ) + ILU: DIRECTIONAL SENSOR ($\theta_T = 45°$)/PSEUDOANALYTICAL RESULTS [20]: AR = 2.45429 AND PD = 22.72801

ℓ	Iterations	CPU time (s)	$\|\bar{r}_k\|_2$	AR	PD
1	306	2429	1.088E-7	2.44961	22.42877
3	201	1659	7.829E-8	2.44959	22.42953
5	185	1522	8.833E-8	2.44954	22.42863
7	189	1555	1.075E-7	2.44961	22.42960
9	180	1628	9.064E-8	2.44958	22.42778
10	180	1626	7.003E-8	2.44960	22.42757

TABLE III
CONVERGENCE OF RGMRES(m) + ILU: CONVENTIONAL SENSOR ($\theta_T = 0°$)/PSEUDOANALYTICAL RESULTS [20]: AR = 2.37753 AND PD = 22.51453

m	Iterations	CPU time (s)	$\|\bar{r}_k\|_2$	AR	PD
1	-	-	-	-	-
5	1107	4745	4.870E-5	2.37185	22.02289
10	331	1479	4.833E-5	2.37206	22.02887
20	148	767	4.831E-5	2.37168	22.00931
30	131	890	4.800E-5	2.37259	22.02423
40	114	775	4.802E-5	2.37459	22.02429

TABLE IV
CONVERGENCE OF RGMRES(m) + ILU: DIRECTIONAL SENSOR ($\theta_T = 45°$)/PSEUDOANALYTICAL RESULTS [20]: AR = 2.45429 AND PD = 22.72801

m	Iterations	CPU time (s)	$\|\bar{r}_k\|_2$	AR	PD
1	-	-	-	-	-
5	3920	18731	5.737E-5	2.44963	22.43550
10	602	2445	5.710E-5	2.44987	22.43071
20	307	1601	5.732E-5	2.44978	22.42438
30	260	1473	5.622E-5	2.44969	22.43117
40	246	2097	5.690E-5	2.44962	22.42465

the discrepancies are below 0.3% for the AR and below 0.5° for the PD. Results listed in Tables III and IV clearly show that RGMRES(m) is sensitive to changes in the RHS, i.e., the convergence deteriorates when the transmitter antenna is tilted. Bi-CGSTAB(ℓ), however, maintains its convergence behavior, showing an advantage over RGMRES(m) in this case.

Even though the algorithms become more expensive with respect to the number of inner products and vector updates as ℓ and m increase, they converge faster, and therefore, the total CPU time needed for a given accuracy actually decreases. The time required for the ILU factorization takes about 15% of the overall CPU time. Note that if m is "too small," RGMRES(m) may be slow to converge or may fail to converge at all. On

TABLE V
ITERATION COUNT VERSUS DROP TOLERANCE

	Conventional sensor ($\theta_T = 0^o$)		Directional sensor ($\theta_T = 45^o$)	
DTOL	Bi-CGSTAB	RGMRES	Bi-CGSTAB	RGMRES
10^{-1}	240	92	330	514
10^{-2}	240	92	330	514
10^{-3}	220	95	280	535
10^{-4}	140	131	180	260
10^{-5}	100	175	120	188
10^{-6}	50	63	60	83

TABLE VI
ITERATION COUNT AND CPU TIME VERSUS ORDER ℓ (Bi-CGSTAB(ℓ) + SSOR)

	Conventional sensor ($\theta_T = 0^o$)		Directional sensor ($\theta_T = 45^o$)	
ℓ	Iterations	CPU time (s)	Iterations	CPU time (s)
1	414	3160	-	-
3	249	2141	-	-
5	215	1812	3225	30567
7	210	1779	-	-
9	198	1693	1242	12210
10	190	1558	1420	13002

the other hand, a value of m that is larger than necessary would cost excessive CPU and require more memory. Here, RGMRES(20) has about the same memory requirements as Bi-CGSTAB(10). Although Bi-CGSTAB(ℓ) converges in a lower number of iterations, RGMRES(m) has a lower computational cost per iteration step and converges faster. Both methods have shown a similar accuracy.

The influence of DTOL on the convergences of Bi-CGSTAB(10) and RGMRES(30) is shown in Table V. As DTOL decreases, RGMRES(30) becomes less sensitive to changes in the RHS. This is expected because, for ill-conditioned problems, a small drop tolerance is usually required to construct a better ILU preconditioner. Moreover, both the CPU time and memory costs required for the factorization step increase, as expected.

The performance of Bi-CGSTAB(ℓ) + SSOR is summarized in Table VI. In contrast to ILU, the SSOR preconditioner can be derived from the coefficient matrix without any work. The overrelaxation parameter is chosen as $\omega = 1.0$. By comparing Tables I and VI, it is seen that ILU outperforms SSOR (about 20% faster) in the conventional logging sensor case. In the directional case, the convergence deteriorates, and SSOR does not converge at all. Fig. 3 shows the number of iterations versus ω for both conventional and directional sensor simulations. The results show that the convergence is highly dependent on the overrelaxation parameter ω in the directional logging sensor case. The value of ω does not appear to have great influence on the convergence of Bi-CGSTAB(ℓ) + SSOR in the conventional logging sensor simulations.

Finally, a 45° deviated borehole in an inhomogeneous formation is considered. The computational grid employs 49 cells in the ρ-direction and 10 cells in the φ-direction. In the z-direction, the number of cells depends on the transmitter depth. The domain along the z-direction is truncated at a distance of twice the skin depth in the formation (that depends on the conductivity) away from both the upper receiver (top boundary)

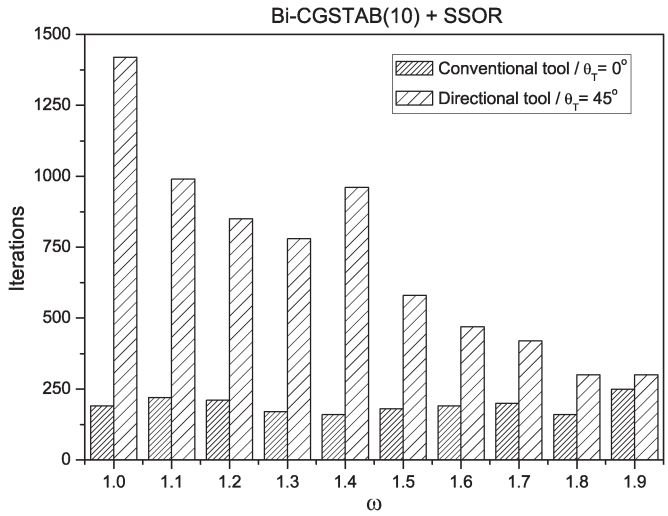

Fig. 3. Iteration count versus overrelaxation parameter ω for Bi-CGSTAB(ℓ) + SSOR algorithm, in both conventional and directional logging sensor simulations.

and the transmitter (bottom boundary). In the radial direction, $\Delta\rho$ varies from 0.635 to 7.12 cm, while in the longitudinal direction, Δz varies from 2.54 to 2.67 cm. Fig. 4(a) and (b) compares the CPU time of conventional and directional logging sensors crossing a three-layer formation with a 60-in-thick dipping (mid-)bed. In these figures, the abscissa represents the distance between the transmitter coil (source) and the interface between the bottom and midlayers. The conductivities of the bottom, mid, and top layers are $\sigma = 1.0, 0.01,$ and 1.0 S/m, respectively. Results for Bi-CGSTAB(10) and RGMRES(30) with both ILU and SSOR preconditioners are shown in Fig. 4, with parameters DTOL $= 10^{-4}$ and $\omega = 1.0$. RGMRES(30) + ILU is the fastest algorithm, taking an average CPU time of 81 and 106 s per logging point for conventional and directional logging sensor simulations, respectively. RGMRES(30) + ILU is about 50% faster than Bi-CGSTAB(10) in the conventional sensor case. For the directional case, the difference decreases to about 20%. When SSOR is used as a preconditioner, the convergences of both algorithms deteriorate. For the directional case, the convergence of RGMRES(30) + SSOR is highly dependent on the source position (i.e., on changes in the RHS). Bi-CGSTAB(10) + SSOR}, however, maintains the number of iterations within acceptable levels, showing a slightly advantage over RGMRES(30) + SSOR.

IV. CONCLUSION

We have compared the convergence behavior of three preconditioned Krylov subspace methods, viz., CGS, RGMRES(m), and Bi-CGSTAB(ℓ) for solving large (non-Hermitian) sparse linear systems arising from the 3-D finite-volume modeling of borehole sensors. Despite being theoretically attractive, CGS is plagued by instabilities in the computed residuals, which affect the convergence in the examples considered here. RGMRES(m) can easily stagnate if the size m of the orthogonal basis is too small or if the preconditioner is not effective. Bi-CGSTAB(ℓ) seems robust and reliable, but it was found to be slower than RGMRES in most cases. On the other hand,

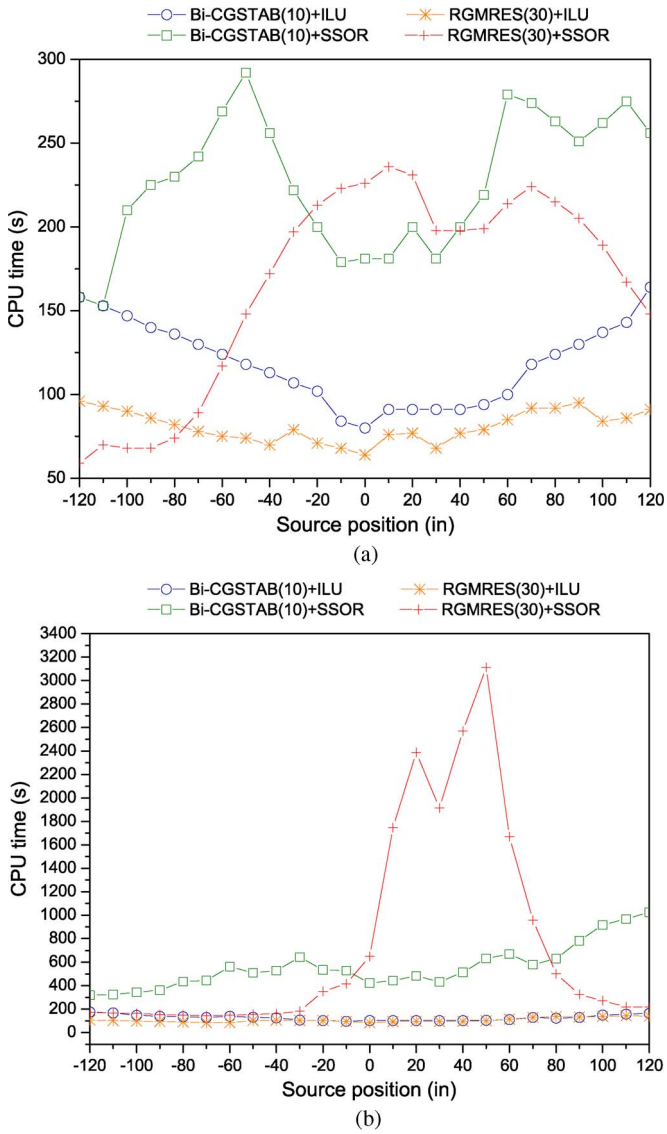

Fig. 4. CPU time versus source position. The abscissa represents the distance between the transmitter coil (source) and the bottom/midlayer interface. The conductivities of the bottom, middle, and top layers are $\sigma = 1.0, 0.01,$ and 1.0 S/m, respectively, and the dipping angle is $(\theta_{\rm dip}) = 45^\circ$. (a) Conventional logging sensor simulation. (b) Directional logging sensor simulation.

RGMRES(m) was found to be considerably more sensitive to changes in the RHS, as opposed to Bi-CGSTAB(ℓ). Although RGMRES(m) and Bi-CGSTAB(ℓ) provide similar numerical accuracy, their convergence rates are highly dependent on the borehole sensor geometry as well as on the type of preconditioning used. In all cases considered here, the ILU preconditioner has outperformed SSOR.

REFERENCES

[1] M. Sato, J. Fuziwara, M. Miyaire, K. Kashihara, and H. Nitsuma, "Directional induction logging methods," in *Proc. SPWLA 35th Annu. Logging Symp.*, Jun. 1994, pp. 1–16.

[2] M. S. Bittar, "Electromagnetic wave resistivity tool having a tilted antenna for determining the horizontal and vertical resistivities and relative dip angle in anisotropic earth formations," U.S. Patent 6 163 155, Dec. 19, 2000.

[3] T. Hagiwara and H. Song, "Directional resistivity measurements for azimuthal proximity detection of bed boundaries," U.S. Patent 6 181 138, Jan. 30, 2001.

[4] Q. Li, D. Omeragic, L. Chou, L. Yang, K. Duong, J. Smits, J. Yang, T. Lau, C. B. Liu, R. Dworak, V. Dreuillault, and H. Ye, "New directional electromagnetic tool for proactive geosteering and accurate formation evaluation while drilling," in *Proc. SPWLA 46th Annu. Logging Symp.*, New Orleans, LA, Jun. 2005.

[5] J. Li and C. Liu, "A three-dimensional transmission line matrix (TLM) method for simulations of logging tools," *IEEE Trans. Geosci. Remote Sens.*, vol. 38, no. 4, pp. 1522–1529, Jul. 2000.

[6] G.-X. Fan, Q. H. Liu, and S. P. Blanchard, "3-D numerical mode-matching (NMM) method for resistivity well-logging tools," *IEEE Trans. Antennas Propag.*, vol. 48, no. 10, pp. 1544–1552, Oct. 2000.

[7] S. Liu and M. Sato, "Electromagnetic logging technique based on borehole radar," *IEEE Trans. Geosci. Remote Sens.*, vol. 40, no. 9, pp. 2083–2092, Sep. 2002.

[8] Z.-Q. Zhang and Q.-H. Liu, "Applications of the BCGS-FFT method to 3-D induction well-logging problems," *IEEE Trans. Geosci. Remote Sens.*, vol. 41, no. 5, pp. 998–1004, May 2003.

[9] G. Gao, C. Torres-Verdin, and S. Fang, "Fast 3D modeling of borehole induction measurements in dipping and anisotropic formations using a novel approximation technique," *Petrophysics*, vol. 45, no. 4, pp. 335–349, Jul./Aug. 2004.

[10] T. Wang and J. Signorelli, "Finite-difference modeling of electromagnetic tool response for logging while drilling," *Geophysics*, vol. 69, no. 1, pp. 152–160, 2004.

[11] Y.-K. Hue, F. L. Teixeira, L. E. San Martin, and M. Bittar, "Modeling of EM logging tools in arbitrary 3-D borehole geometries using PML-FDTD," *IEEE Geosci. Remote Sens. Lett.*, vol. 2, no. 1, pp. 78–81, Jan. 2005.

[12] Y.-K. Hue, F. L. Teixeira, L. E. San Martin, and M. Bittar, "Three-dimensional simulation of eccentric LWD tool response in boreholes through dipping formations," *IEEE Trans. Geosci. Remote Sens.*, vol. 43, no. 2, pp. 257–268, Feb. 2005.

[13] Y.-K. Hue and F. L. Teixeira, "Analysis of tilted-coil eccentric borehole antennas in cylindrical multilayered formations for well-logging applications," *IEEE Trans. Antennas Propag.*, vol. 54, no. 4, pp. 1058–1064, Apr. 2006.

[14] D. Pardo, C. Torres-Verdin, and L. F. Demkowicz, "Simulation of multifrequency borehole resistivity measurements through a metal casing using a goal-oriented hp finite-element method," *IEEE Trans. Geosci. Remote Sens.*, vol. 44, no. 8, pp. 2125–2134, Aug. 2006.

[15] Y.-K. Hue and F. L. Teixeira, "Numerical mode-matching method for tilted-coil antennas in cylindrically layered anisotropic media with multiple horizontal beds," *IEEE Trans. Geosci. Remote Sens.*, vol. 45, no. 8, pp. 2451–2462, Aug. 2007.

[16] H. O. Lee and F. L. Teixeira, "Cylindrical FDTD analysis of LWD tools through anisotropic dipping-layered earth media," *IEEE Trans. Geosci. Remote Sens.*, vol. 45, no. 2, pp. 383–388, Feb. 2007.

[17] D. Wu, J. Chen, and C. R. Liu, "An efficient FDTD method for axially symmetric LWD environments," *IEEE Trans. Geosci. Remote Sens.*, vol. 46, no. 6, pp. 1652–1656, Jun. 2008.

[18] M. S. Novo, L. C. da Silva, and F. L. Teixeira, "Finite volume modeling of borehole electromagnetic logging in 3-D anisotropic formations using coupled scalar-vector potentials," *IEEE Antennas Wireless Propag. Lett.*, vol. 6, pp. 549–552, 2007.

[19] M. S. Novo, L. C. da Silva, and F. L. Teixeira, "Comparison of coupled-potentials and field-based finite-volume techniques for modeling of borehole EM tools," *IEEE Geosci. Remote Sens. Lett.*, vol. 5, no. 2, pp. 209–211, Apr. 2008.

[20] M. S. Novo, L. C. da Silva, and F. L. Teixeira, "Three-dimensional finite-volume analysis of directional resistivity logging tools," *IEEE Trans. Geosci. Remote Sens.*, vol. 48, no. 3, pp. 1151–1158, Mar. 2010.

[21] Y. Saad, *Iterative Methods for Sparse Linear Systems*. Boston, MA: PWS-Kent, 1995.

[22] R. Barrett, M. Berry, T. F. Chan, J. Demmel, J. Donato, J. Dongarra, V. Eijkhout, R. Pozo, C. Romine, and H. Van der Vorst, *Templates for the Solution of Linear Systems: Building Blocks for Iterative Methods*. Philadelphia, PA: SIAM, 1994.

[23] W. Arnoldi, "The principle of minimized iterations in the solution of the matrix eigenvalue problem," *Q. Appl. Math.*, vol. 9, no. 1, pp. 17–29, 1951.

[24] H. A. van der Vorst, "Bi-CGSTAB: A fast and smoothly converging variant of Bi-CG for the solution of nonsymmetric linear systems," *SIAM J. Sci. Stat. Comput.*, vol. 13, no. 2, pp. 631–644, Mar. 1992.